

This discussion paper is/has been under review for the journal *Atmospheric Chemistry and Physics (ACP)*. Please refer to the corresponding final paper in *ACP* if available.

**The spatial
distribution of the
reactive iodine
species IO**

K. Seitz et al.

The spatial distribution of the reactive iodine species IO from simultaneous active and passive DOAS observations

K. Seitz¹, J. Buxmann¹, D. Pöhler¹, T. Sommer^{1,*}, J. Tschirter¹, C. O'Dowd², and U. Platt¹

¹Institute of Environmental Physics, University of Heidelberg, Im Neuenheimer Feld 229, 69120 Heidelberg, Germany

²School of Physics & Centre for Climate & Air Pollution Studies, Environmental Change Institute National University of Ireland, Galway, University Road, Galway, Ireland

* now at: Eawag, Limnological Research Center, Seestr. 79, Kastanienbaum, Switzerland

Received: 19 August 2009 – Accepted: 18 September 2009 – Published: 12 October 2009

Correspondence to: K. Seitz (katja.seitz@iup.uni-heidelberg.de)

Published by Copernicus Publications on behalf of the European Geosciences Union.

Title Page

Abstract

Introduction

Conclusions

References

Tables

Figures

⏪

⏩

◀

▶

Back

Close

Full Screen / Esc

Printer-friendly Version

Interactive Discussion

Abstract

We present investigations of the reactive iodine species (RIS) IO, OIO and I₂ in a coastal region from a field campaign simultaneously employing active long path differential optical absorption spectroscopy (LP-DOAS) as well as passive multi-axis differential optical absorption spectroscopy (MAX-DOAS). The campaign took place at the Martin Ryan Institute (MRI) in Carna, County Galway at the Irish West Coast about 6 km south-east of the atmospheric research station Mace Head in summer 2007. In order to study the horizontal distribution of the trace gases of interest, we established two almost parallel active LP-DOAS light paths, the shorter of 1034 m length just crossing the intertidal area, whereas the longer one of 3946 m length also crossed open water during periods of low tide. In addition we operated two passive Mini-MAX-DOAS instruments with the same viewing direction. While neither OIO nor I₂ could be unambiguously identified with any of the instruments, IO could be detected with active as well as passive DOAS. The IO column densities seen at both active LP-DOAS light paths are almost the same. Thus it can be concluded that coastal IO is almost exclusively located in the intertidal area, where we detected mixing ratios of up to 35±7.7 ppt (equivalent to pmol/mol). Nucleation events with particle concentrations of 10⁶ cm⁻³ particles were observed each day correlating with high IO mixing ratios. Therefore we feel that our detected IO concentrations confirm the results of model studies, which state that in order to explain such particle bursts, IO mixing ratios of 50 to 100 ppt in so called “hot-spots” are required.

1 Introduction

It is well known that reactive halogen species (RHS) affect tropospheric chemistry in different ways. A drastic example is the total depletion of boundary layer ozone in polar spring within days or hours by catalytic cycles involving bromine (see e.g., von Glasow and Crutzen, 2007; Simpson et al., 2007 and references therein). While the

The spatial distribution of the reactive iodine species IO

K. Seitz et al.

Title Page

Abstract

Introduction

Conclusions

References

Tables

Figures

⏪

⏩

◀

▶

Back

Close

Full Screen / Esc

Printer-friendly Version

Interactive Discussion

**The spatial
distribution of the
reactive iodine
species IO**

K. Seitz et al.

[Title Page](#)[Abstract](#)[Introduction](#)[Conclusions](#)[References](#)[Tables](#)[Figures](#)[⏪](#)[⏩](#)[◀](#)[▶](#)[Back](#)[Close](#)[Full Screen / Esc](#)[Printer-friendly Version](#)[Interactive Discussion](#)

destruction of arctic boundary ozone appears to be mainly driven by BrO (with minor contributions from IO and ClO), at mid latitudes and possibly in Antarctica (Frieß et al., 2001; Saiz-Lopez et al., 2008) IO plays an important role in the process of ozone destruction. Besides its influence on the ozone budget, reactive iodine (like reactive bromine) affects atmospheric chemistry by changing the NO/NO₂ and OH/HO₂ partitioning (e.g., Platt and Hönniger, 2003). Additionally, recent field studies, mainly carried out at Mace Head atmospheric research station (Mace Head) (e.g., O'Dowd et al., 2002; Mäkelä et al., 2002) indicate that reactive iodine plays a key role in the formation of new particles in coastal areas. This phenomenon has been studied in several laboratory experiments (e.g., Hoffmann et al., 2001; Jimenez et al., 2003; Burkholder et al., 2004; McFiggans et al., 2004; Palmer et al., 2005) and model studies (e.g., Pechtl et al., 2006; Saiz-Lopez et al., 2006a; Vuollekoski et al., 2009). A review of the current knowledge on marine aerosol production can be found in O'Dowd and de Leeuw (2007). If those particles grow to become cloud condensation nuclei (CCN), they could influence cloud properties and therefore have an impact on climate.

The most likely source of reactive iodine is the photolysis of molecular iodine and organohalogens emitted by macroalgae. While initially organohalogens, especially the short-lived diiodomethane CH₂I₂ were assumed to be the major precursors of reactive iodine, at the reported levels of I₂ and CH₂I₂, the former would constitute the dominating source of RHS.

Most of the measurements of RHS at coastal sites were conducted at Mace Head (e.g., Alicke et al., 1999; Hebestreit, 2001; Saiz-Lopez and Plane, 2004; Saiz-Lopez et al., 2004a, 2006a,b; Peters et al., 2005; Bale et al., 2008), which is located about 6 km North-West of the MRI. A summary of the thitherto made observations of RHS can be found in Peters et al. (2005).

All above mentioned measurements were carried out using active LP-DOAS. Since the thus obtained mixing ratios are an average along kilometer-long light paths, one has to keep in mind that a possibly inhomogeneous distributions of the trace gases can not be resolved. Burkholder et al. (2004) state that the mixing ratios derived from long

path absorption measurements are too low to account for the large aerosol production observed. They suggest an inhomogeneous source distribution resulting in areas with much above average IO mixing ratios, so-called “hot-spots”, to explain the significant particle formation. They conclude that their hypothesis has to be confirmed by further field studies.

In this study we present results from active LP-DOAS measurements of RIS on two almost parallel light paths of different lengths (1034 m and 3946 m), where the shorter light path was just crossing intertidal area, in order to obtain information about the source distribution.

The first section addresses the instrument set-up and the measurement site, followed by a description of the DOAS analysis. In the second section results will be presented and discussed. We conclude with a summary and an outlook.

2 Experimental

2.1 The active LP-DOAS system

DOAS (Platt and Perner, 1983; Platt and Stutz, 2008) is a well established technique to identify and quantify trace gases by their narrow band absorption structures. In this study we used an active LP-DOAS instrument for the detection of the following RIS: IO, OIO and I_2 . The setup of the LP-DOAS system used was a further development of the coaxial mirror system introduced by Axelson et al. (1990). The light of a high pressure Xe-arc lamp of the type XBO500 (Osram) was collimated into six transmitting fibres of a Y-fibre bundle. The bundle at the telescope side consists of one receiving fibre surrounded by the six transmitting fibres. The transmitting fibres illuminate the mirror of the telescope yielding an almost parallel light beam, the receiving fibre is connected to the spectrometer. A detailed description of the Fibre LP-DOAS can be found in Merten et al. (2009); Merten (2008). The almost parallel light beam is then alternately sent on two different light paths through the open atmosphere to two

The spatial distribution of the reactive iodine species IO

K. Seitz et al.

Title Page

Abstract

Introduction

Conclusions

References

Tables

Figures

⏪

⏩

◀

▶

Back

Close

Full Screen / Esc

Printer-friendly Version

Interactive Discussion

arrays of quartz prism retro-reflectors (63 mm diameter each) located at distances of 1973 m and 517 m. The number of quartz prisms in the arrays was 39 and 13, respectively. The reflected light was transmitted to an Acton 500pro spectrometer ($f = 6.9$, 600 gr/mm grating, thermostated to 25°C) via the receiving fibre of the fibre bundle, where it was analyzed. A reference spectrum was taken before and after each measurement spectrum using a shortcut system consisting of an aluminium diffuser plate that was placed several mm in front of the fibre bundle thus recording a lamp spectrum without passage through the atmosphere. The detector was a 1024 pixel photodiode array detector (type Hamamatsu S3904-1024). The resulting spectral resolution was about 0.5 nm FWHM. Four different wavelength ranges were successively covered to measure the trace gases of interest: BrO in 320 ± 40 nm, IO in 430 ± 40 nm, OIO and I_2 in 550 ± 40 nm and NO_3 in 640 ± 40 nm. The latter measurements were only performed at solar zenith angles $> 85^{\circ}$. These wavelength ranges also cover other species, such as O_3 , NO_2 , H_2O , O_4 , SO_2 , HONO and HCHO, which were taken into account for the analysis. The analysis procedure itself will be described in Sect. 3.

2.2 The passive MAX-DOAS systems

In addition to the active instrument, two passive MAX-DOAS instruments were applied to detect RIS. The MAX-DOAS technique was already described in detail (e.g., Hönninger and Platt, 2002; Hönninger et al., 2004). The instruments used, were “Mini-MAX-DOAS-devices” (Bobrowski et al., 2003). Scattered sunlight is focussed by a quartz lens ($f = 40$ mm, $d = 20$ mm, aperture angle $< 0.6^{\circ}$) and transmitted to a miniature crossed Czerny-Turner spectrometer/detector unit (“USB2000”, Ocean Optics, Inc.) via a fibre bundle. The whole set up is placed in a sealed, weatherproof aluminium box which also contained the peltier cooler to stabilize the spectrometer to 0°C . An attached stepper motor allows the instrument to observe scattered sunlight at a series of different elevation angles. The whole instrument was controlled by PC via USB connection. The two instruments covered the fixed wavelength ranges 325–461 nm for the detection of BrO and IO and 538–635 nm for OIO and I_2 , respectively. Their viewing

The spatial distribution of the reactive iodine species IO

K. Seitz et al.

Title Page

Abstract

Introduction

Conclusions

References

Tables

Figures

⏪

⏩

◀

▶

Back

Close

Full Screen / Esc

Printer-friendly Version

Interactive Discussion



azimuth was set up almost parallel to the light paths of the active instrument. Spectra were taken under 2°, 4°, 6°, 10°, 20° and 90° elevation angle.

2.3 Site description

Between 3 August and 9 September 2007, an intensive field campaign was conducted at the Martin Ryan Institute (MRI) in Carna (53.31° N, 9.83° W) at the Irish West Coast, about 6 km south-east from Mace Head. A description of the area around Carna can be found in e.g. Hebestreit (2001). The MRI is located in front of Mweenish Island, an island with a very high seaweed density (see Fig. 1). Due to its high seaweed density in all wind directions, the area has already been object of earlier field measurements (e.g., Sellegri et al., 2005).

During the campaign the wind direction was almost all the time North/North-West. The weather was sunny during most of the days, with just few rainy days. Due to the sunny weather and the vast seaweed abundance, particle bursts were observed almost each day. An example for such a particle burst observed at 1 September can be found in Fig. 2. We concentrate on a core period of five days of measurements between 30 August and 4 September. Of the five days of observation, 31 August and 2 September were rainy, whereas the other three days were sunny and partly cloudy but with no rain and good visibility. During the five days a maximal tidal range of 4.4 m was observed.

The instruments were positioned at few meters distance from the waterfront during high tide. The light beam of the active LP-DOAS instrument was crossing the water at an altitude of about 5 m above sea level at high tide. During low tide the water below the short absorption path was completely removed, whereas the long light path crossed the same intertidal area first, then the sea and again an intertidal area in front of Finish Island, where the second retro-reflector was placed. Figure 1 shows the area of the MRI and the absorption paths. It can be seen, that due to the slight angle between the two light paths, the long light path crosses less intertidal area in front of the instrument. Figure 3 demonstrates that the seaweed of the area is mainly dominated by the type *Laminaria*, which are known to be strong emitters of I₂ as well as halocarbons (e.g.,

The spatial distribution of the reactive iodine species IO

K. Seitz et al.

Title Page

Abstract

Introduction

Conclusions

References

Tables

Figures



Back

Close

Full Screen / Esc

Printer-friendly Version

Interactive Discussion



3 DOAS data analysis

3.1 Active LP-DOAS

For the analysis of the LP-DOAS spectra the software DOASIS (Kraus (2005)) was used to simultaneously fit the different references to the atmospheric spectrum using a non-linear least-squares method (e.g., Stutz and Platt, 1996). Laboratory studies previous to the campaign showed that the detection limit of the instrument could be improved by taking reference spectra of the light source as close in time to the measurement spectrum as possible (Buxmann, 2008). Therefore two lamp reference spectra (shortcut spectra), one directly before and one directly after the measurement spectrum, were recorded, added and included in the fit. In addition a polynomial was included to account for broad band structures due to scattering in the atmosphere. On the basis of Stutz and Platt (1996) the statistical error of our analysis was multiplied by a factor 2, to obtain the real measurement error. The detection limit is estimated by multiplying a factor 2 to the 1σ statistical error.

IO was analyzed in the wavelength range between 416 and 448.5 nm where four of the strongest absorption bands of the electronic transition $A^2\Pi_{3/2} \leftarrow X^2\Pi_{3/2}$ are. Due to large structures in the residual arising from the Xe-lamp, the wavelength range between 442 nm and 444 nm was excluded from the fit. In addition to the IO cross section a reference of NO_2 was included in the fit procedure. Table 1 summarizes the absorption cross sections used in this work. The polynomial included was of 5th order. Figure 4 shows a sample evaluation of 30 August 2007, 14:26 UTC, taken on the long light path. The spectrum corresponds to a column density of $(8.83 \pm 0.85) \times 10^{13}$ molec/cm². Assuming homogenous mixing along the 3946 m light path, this would correspond to a mixing ratio of (8.9 ± 0.86) ppt.

The evaluation of OIO and I_2 was performed in the wavelength range between 530

The spatial distribution of the reactive iodine species IO

K. Seitz et al.

Title Page

Abstract

Introduction

Conclusions

References

Tables

Figures

⏪

⏩

◀

▶

Back

Close

Full Screen / Esc

Printer-friendly Version

Interactive Discussion



and 567 nm. This covers 6 vibrational bands of OIO and 15 bands of the electronic transition $B^3\Pi(0_u^+) - X^1\Sigma_g^+$ of I_2 . Besides the cross sections of OIO and I_2 , references of NO_2 , O_4 and H_2O and a 4th order polynomial were included in the fit.

3.2 MAX-DOAS

For the evaluation of the MAX-DOAS measurements the software WinDOAS (Fayt and van Rozendael, 2001) was used to perform a non-linear least-squares fit. A description of the evaluation procedure can be found in Hönninger and Platt (2002). To detect the absorbers of interest, a 90° reference spectrum of the same sequence, a ring spectrum and cross sections of all other absorbers were fitted to the atmospheric spectrum. The results of the evaluation are therefore “differential slant column densities” (dSCDs), i.e. $S_{dSCD} = S(\alpha) - S(90^\circ)$, where S denotes the signal of the respective absorber [molec/cm^2] and α the elevation angle. An overview of the MAX-DOAS analysis setting applied is given in Table 2.

4 Results and discussion

4.1 MAX-DOAS measurements

During the five days of observation OIO and I_2 could not be detected with the MAX-DOAS instruments. While the analysis yielded periods where the differential slant column densities (dSCDs) exceeded the detection limit, which was for the 2° angle on average $1.4 \times 10^{14} \text{ molec}/\text{cm}^2$ for OIO and $5.6 \times 10^{14} \text{ molec}/\text{cm}^2$ for I_2 , the results did not withstand different sensitivity studies: A change of the analysis wavelength range to 547–567 nm changed the results as significantly as changing the order of the polynomial to 2 or changing the offset to first order. Similar problems for the detection of OIO and I_2 with the Mini-MAX-DOAS instruments were reported before (e.g., Stein, 2006; Martin, 2007).

The spatial distribution of the reactive iodine species IO

K. Seitz et al.

Title Page

Abstract

Introduction

Conclusions

References

Tables

Figures

⏪

⏩

◀

▶

Back

Close

Full Screen / Esc

Printer-friendly Version

Interactive Discussion

The spatial distribution of the reactive iodine species IO

K. Seitz et al.

On all five days IO exceeded the average detection limit of 2.8×10^{13} molec/cm², also sensitivity studies indicated the results to be robust. The maximum dSCD observed was 1.0×10^{14} molec/cm² (Fig. 5). While under an elevation angle of 2° the dSCDs are very high, especially around low tide, the dSCDs decreases rapidly for higher elevation angles. This indicates a strong vertical gradient in the IO concentration. This is in contrast to the studies of Stutz et al. (2007) in the Gulf of Maine (Appledore Island), who did not observe a separation between the elevation angles. They concluded that this could be due to their measurement just probing a single IO plume at a certain height and distance, where a vertical gradient would not be reflected in the results. Since our instrument was located just a few meters above sea level and from the algae field whereas the instrument in Appledore Island was located about 20 m above sea level, we probably measured the vertical gradient directly.

4.2 LP-DOAS measurements

OIO could not be identified unambiguously during the 5 days. Even though the column densities exceed the statistical 2σ detection limit (1.2×10^{14} molec/cm² or ≈ 12 ppt on the long and 1.8×10^{14} molec/cm² or ≈ 70 ppt on the short light path) several times by up to a factor of 2, the fact that the analysis shows strong scattering and yields negative column densities of the same order of magnitude as the positive values (up to about -4×10^{14} molec/cm² on the short, and -5×10^{14} molec/cm² on the long light path) makes the interpretation difficult. Although the analysis was stable using different fit parameters, no further conclusions about the horizontal distributions can be drawn at this time.

Since I₂ is evaluated in the same spectral wavelength range as OIO, its evaluation shows the same problems. Again, the column densities exceed the statistically derived detection limit several times by about a factor of 2, but due to the short light path, the results show a strong scattering also towards negative column densities. As for OIO the analysis proved to be stable, but anyway no conclusions about the horizontal

[Title Page](#)[Abstract](#)[Introduction](#)[Conclusions](#)[References](#)[Tables](#)[Figures](#)[⏪](#)[⏩](#)[◀](#)[▶](#)[Back](#)[Close](#)[Full Screen / Esc](#)[Printer-friendly Version](#)[Interactive Discussion](#)

distribution can be derived. The average detection limit was 4.9×10^{14} molec/cm² or ≈ 50 ppt on the long light path and 7.3×10^{14} molec/cm² or ≈ 282 ppt on the short light path. The maximum in negative column densities obtained from the evaluation was about -5.5×10^{15} molec/cm² and -8.9×10^{14} molec/cm², respectively.

Figure 6 shows the time series of IO column densities on both light paths (black stars: long light path, blue triangles: short light path). The blue line indicates tidal height and the grey shaded areas mark the periods of darkness. The peaks in IO are correlated to minima in tidal height and maxima in solar radiation. This was also observed during earlier campaigns at Mace Head (e.g., Alicke et al., 1999; Saiz-Lopez et al., 2006b), and also at the French Atlantic Coast (Peters et al., 2005). Stutz et al. (2007) saw no dependence of the IO signal on tidal height, which is so far unexplained.

A striking feature is the observation that the column densities on the long light path are about the same as on the short one with some differences. This is a strong indication that the signal comes to a large fraction from the intertidal area. Converting the maximum IO column density $(9.1 \pm 2.0) \times 10^{13}$ molec/cm² of the short light path into mixing ratios, assuming 1034 m path length and homogenous mixing, yields (35 ± 7.7) ppt. This is in good agreement with not only in-situ measurements carried out with a laser-induced fluorescence instrument at the intertidal area in front of Mace Head during the 30 August 2007 (max. about 20 ppt, R. Commane, University of Leeds, personal communication, 2007), but also with modelling studies (Burkholder et al., 2004). The latter state that 50 to 100 ppt of IO are needed to explain nucleation events with particle concentration of 10^6 cm⁻³ similar to those that were observed each of the 5 days (T. Neary, University of Galway, personal communication, 2007). The reason that our IO signal is still below the necessary 50–100 ppt, that are needed, might be the strong vertical gradient, we see in the MAX-DOAS data. As our light path crosses the seaweed at several meters height, the concentration further down, are probably significantly higher.

We also feel that we can explain the slight differences in the column densities seen at the two light paths. On 30 August we started measurements on the short light path at 14:13 GMT. Until 2 September, the column densities are about the same. On 3

The spatial distribution of the reactive iodine species IO

K. Seitz et al.

Title Page

Abstract

Introduction

Conclusions

References

Tables

Figures

⏪

⏩

◀

▶

Back

Close

Full Screen / Esc

Printer-friendly Version

Interactive Discussion

The spatial distribution of the reactive iodine species IO

K. Seitz et al.

Title Page

Abstract

Introduction

Conclusions

References

Tables

Figures

⏪

⏩

◀

▶

Back

Close

Full Screen / Esc

Printer-friendly Version

Interactive Discussion

September the column density of the short light path exceeds the column density of the long light path by about 50%. This is not due to a change in wind direction (same wind direction on 30 August and 3 September), but because of the slightly different light paths and because of different sources. Figure 1 shows that the long light path crosses less intertidal area in front of the instrument due to a slight angle between the viewing directions. Figure 7 illustrates the LP-DOAS measurement set-up for different water levels. While the intertidal area below the short light path is exposed to ambient air during low tide for all days, due to the steep coast-line, more intertidal area in front of Finish Island is exposed close to low spring tide (30 August). During spring tide the deep water sea weed *Laminaria Digitata* exposed in front of Finish Island probably makes up the difference in column densities due to the shorter fraction of intertidal area at the MRI for the long light path, whereas the following days its IO input decreases. Note that in the afternoon of 31 August, the fibre had to be exchanged. The fact that the light could not be as well mixed with the spare fibre might be responsible for a shift towards negative values afterwards. Therefore the column densities observed after 31 August, 14:00 might be underestimated.

Figure 8 shows a comparison of the 2° and 4° MAX-DOAS IO dSCDs (blue stars and black circs, respectively) with the column densities of the LP-DOAS instrument (long light path: black crosses, short light path: pink triangles). While in principle the data correlate well, it can be seen that the MAX-DOAS dSCDs are generally higher than the LP-DOAS column densities.

Figure 9 shows the correlation between the 2° MAX-DOAS dSCDs and the LP-DOAS column density along the long light path. The data show strong scattering but although the intertidal area in front of the instrument is crossed just once, the MAX-DOAS shows higher column densities most of the time. This is mainly during low tide which is reflected in Fig. 8. The fact that the MAX-DOAS detects a higher signal during periods of low tide indicates that there are additional sources of IO signal for the passive instrument, such as backscattering from the ground through a strong gradient or strong emitting deep-water seaweed behind Finish Island.

The spatial distribution of the reactive iodine species IO

K. Seitz et al.

Title Page

Abstract

Introduction

Conclusions

References

Tables

Figures

⏪

⏩

◀

▶

Back

Close

Full Screen / Esc

Printer-friendly Version

Interactive Discussion

As we know from the LP-DOAS results, the IO signal comes almost exclusively from the intertidal area, which means that the MAX-DOAS signal originates not only from the intertidal zone in front of the MRI, but also from intertidal area further away. If the IO was located only in the intertidal area, its lifetime must be very short. This also means that its concentration should decrease rapidly with height which is in good agreement with the strong decrease of the IO dSCDs towards higher elevation angles. But this also means that the additional signal, the MAX-DOAS detects (its light path only crosses the intertidal area in front of the MRI once) most likely does not come from too far away, as even for 2° elevation after 2 km, the instrument looks at a height of 70 m (see Fig. 7). There are probably two sources, which explain the higher MAX-DOAS signal: First, it probably also probes the intertidal area on the other side of Finish Island. Figure 3 shows that in the deeper water behind Finish Island *Laminaria Hyperborea* is located, which is a very strong emitter of iodine precursors and second, it could be possible, that light reflected from the surface and therefore passing very high concentrations, causes the higher signal.

5 Conclusions

During this study OIO and I₂ could not be observed above the detection limit for both light paths and both techniques. Therefore no information about their horizontal distribution could be obtained and more measurements with longer absorption paths and better detection limits just crossing intertidal area are needed.

IO could clearly be detected, with the observation angle dependence of the observed dSCDs indicating a strong vertical gradient in the IO concentration. The LP-DOAS study also shows that IO is inhomogenously mixed along the light path and that the IO signal is very probably almost exclusively coming from the intertidal area. We feel that we can confirm the so-called “hot-spot-theory” (e.g., Burkholder et al., 2004), that was introduced to explain the formation of nucleation events as they have also been observed during this study.

Acknowledgements. This work was conducted under the MAP Project funded by the European Commission (under FP6 project number 018332). We thank the staff of MRI Carna, especially Richard Fitzgerald, for providing space and support during the campaign. We thank Roland von Glasow for helpful discussions. The efforts of Tom Neary and Darius Ceburnis from NUIG are gratefully acknowledged. We also would like to thank Stefan Kraan from the Irish Seaweed Center for providing seaweed maps.

References

- Alicke, B., Hebestreit, K., Stutz, J., and Platt, U.: Iodine oxide in the marine boundary layer, *Nature*, 397, 572–573, 1999. 21373, 21380
- Axelson, H., Galle, B., Gustavson, K., Ragnarsson, P., and Rudin, M.: A Transmitting / Receiving Telescope for DOAS-Measurements using Retroreflektor Technique, *Techn. Dig. Ser.*, 4, 641–644, 1990. 21374
- Bale, C., Ingham, T., Commane, R., Heard, D., and Bloss, W.: Novel measurements of atmospheric iodine species by resonance fluorescence, *J. Atmos. Chem.*, 60, 51–70, 2008. 21373
- Bloss, W. J., Rowley, D. M., Cox, R. A., and Jones, R. L.: Kinetics and Products of the IO Self-Reaction, *J. of Phys. Chem. A*, 105, 7840–7854, 2001. 21388
- Bobrowski, N., Hönninger, G., Galle, B., and Platt, U.: Detection of bromine monoxide in a volcanic plume, *Nature*, 423, 273–276, 2003. 21375
- Bogumil, K., Orphal, J., Homann, T., Voigt, S., Spietz, P., Fleischmann, O., Vogel, A., Hartmann, M., Bovensmann, H., Frerick, J., and Burrows, J.: Measurements of molecular absorption spectra with the SCIAMACHY pre-flight model: Instrument characterization and reference data for atmospheric remote sensing in the 230–2380 nm region., *J. Photochem. Photobiol.*, 157, 167–184, 2003. 21388
- Burkholder, J. B., Curtius, J., Ravishankara, A. R., and Lovejoy, E. R.: Laboratory studies of the homogeneous nucleation of iodine oxides, *Atmos. Chem. Phys.*, 4, 4943–4988, 2004. 21373, 21380, 21382
- Buxmann, J.: Optimierte Langpfad-DOAS Messungen von BrO und ClO an der irischen Westküste, Diploma thesis, Institut für Umweltphysik, Universität Heidelberg, Germany, 123 pp., 2008. 21377

The spatial distribution of the reactive iodine species IO

K. Seitz et al.

Title Page

Abstract

Introduction

Conclusions

References

Tables

Figures

⏪

⏩

◀

▶

Back

Close

Full Screen / Esc

Printer-friendly Version

Interactive Discussion

- Carpenter, L., Liss, P., Platt, U., and Hebestreit, K.: Coastal zone production of IO precursors: a 2-dimensional study, *Atmos. Chem. Phys.*, 1, 9–17, 2001. 21377
- Fayt, C. and van Rozendael, M.: WinDOAS, iSAB/BIRA Belgium, <http://www.oma.be/BIRA-IASB>, 2001. 21378
- 5 Frieß, U., Wagner, T., Pundt, I., Pfeilsticker, K., and Platt, U.: Spectroscopic Measurements of Tropospheric Iodine Oxide at Neumeyer Station, Antarctica, *Geophys. Res. Lett.*, 28, 1941–1944, 2001. 21373
- Greenblatt, G. D., Orlando, J. J., Burkholder, J. B., and Ravishankara, A. R.: Absorption Measurements of Oxygen between 330 and 1140 nm, *J. Geophys. Res.*, 95, 18577–18582, 1990. 21388
- 10 Hebestreit, K.: Halogen Oxides in the Mid-Latitudinal Planetary Boundary Layer, Ph.D. thesis, Institut für Umweltphysik, Universität Heidelberg, Germany, 2001. 21373, 21376
- Hoffmann, T., O'Dowd, C. D., and Seinfeld, J. H.: IO homogeneous nucleation: An explanation for coastal new particle formation, *Geophys. Res. Lett.*, 28, 1949–1952, 2001. 21373
- 15 Hönninger, G. and Platt, U.: Observations of BrO and its vertical distribution during surface ozone depletion at Alert, *Atmos. Environ.*, 36, 2481–2489, 2002. 21375, 21378
- Hönninger, G., von Friedeburg, C., and Platt, U.: Multi axis differential optical absorption spectroscopy (MAX-DOAS), *Atmos. Chem. Phys.*, 4, 231–254, 2004. 21375
- Jimenez, J. L., Bahreini, R., Cocker, D. R., Zhuang, H., Varutbangkul, V., Flagan, R. C., Seinfeld, J. H., O'Dowd, C. D., and Hoffmann, T.: New particle formation from photooxidation of diiodomethane CH₂I₂, *J. Geophys. Res.*, 108(D10), 4318, doi:10.1029/2002JD002452, 2003. 21373
- 20 Kraus, S.: DOASIS A Framework Design for DOAS, Ph.D. thesis, Combined Faculties for Mathematics and for Computer Science, University of Mannheim, Germany, 2005. 21377
- 25 Mäkelä, J. M., Hoffmann, T., Holzke, C., Väkevä, M., Suni, T., Mattila, T., Aalto, P. P., Tapper, U., Kauppinen, E. I., and O'Dowd, C. D.: Biogenic iodine emissions and identification of end-products in coastal ultrafine particles during nucleation bursts, *J. Geophys. Res.*, 107(D19), 8110, doi:10.1029/2001JD000580, 2002. 21373
- Martin, M.: Measurements of Halogen Oxide Radicals over the North Atlantic, Diploma thesis, Institut für Umweltphysik, Universität Heidelberg, Germany, 2007. 21378
- 30 McFiggans, G., Coe, H., Burgess, R., Allan, B. J., Cubison, M., Rami Alfarra, M., Saunders, R., Saiz-Lopez, A., Plane, J. M. C., Wevill, D., Carpenter, L., Rickard, A. R., and Monks, P. S.: Direct evidence for coastal iodine particles from *Laminaria* macroalgae – linkage to

The spatial distribution of the reactive iodine species IO

K. Seitz et al.

Title Page

Abstract

Introduction

Conclusions

References

Tables

Figures

◀

▶

◀

▶

Back

Close

Full Screen / Esc

Printer-friendly Version

Interactive Discussion

- emissions of molecular iodine, *Atmos. Chem. Phys.*, 4, 701–713, 2004. 21373, 21377
- Merten, A.: Neues Design von Langpfad-DOAS-Instrumenten basierend auf Faseroptiken und Anwendungen der Untersuchung der urbanen Atmosphäre, Ph.D. thesis, University of Heidelberg, Germany, 2008. 21374
- 5 Merten, A., Tschritter, J., and Platt, U.: Novel design of DOAS-long-path telescopes based on fiber optics, *Appl. Opt.*, submitted, 2009. 21374
- O'Dowd, C. and de Leeuw, G.: Marine aerosol production: a review of the current knowledge, *Phil. Trans. R. Soc. A*, 365, 1753–1774, doi:10.1098/rsta2007.2043, 2007. 21373
- O'Dowd, C. D., Hämeri, K., Mäkelä, J., Pirjola, L., Kulmala, M., Jennings, S., Berresheim, H.,
10 Hansson, H.-C., de Leeuw, G., Kunz, G., Allen, A., Hewitt, C., Jackson, A., Viisanen, Y.,
and Hoffmann, T.: A dedicated study of New Particle Formation and Fate in the Coastal Environmnet (PARFORCE): Overview of objectives and achievements, *J. Geophys. Res.*, 107(D19), 8108, doi:10.1029/2001JD000555, 2002. 21373
- Palmer, C., Anders, T., Carpenter, L., Küpper, F., and McFiggans, G.: Iodine and Halocarbon
15 Response of *Laminaria digitata* to Oxidative Stress and Links to Atmospheric New Particle
Production, *Environ. Chem.*, 2, 282–290, doi:10.1071/EN05078, 2005. 21373
- Pechtl, S., Lovejoy, E. R., Burkholder, J. B., and von Glasow, R.: Modeling the possible role of
iodine oxides in atmospheric new particle formation, *Atmos. Chem. Phys.*, 6, 503–523, 2006,
<http://www.atmos-chem-phys.net/6/503/2006/>. 21373
- 20 Peters, C., Pechtl, S., Stutz, J., Hebestreit, K., Hönninger, G., Heumann, K. G., Schwarz, A.,
Winterlik, J., and Platt, U.: Reactive and organic halogen species in three different European
coastal environments, *Atmos. Chem. Phys.*, 5, 3357–3375, 2005,
<http://www.atmos-chem-phys.net/5/3357/2005/>. 21373, 21380
- Platt, U. and Hönninger, G.: The role of halogen species in the troposphere, *Chemosphere*, 52,
25 325–338, 2003. 21373
- Platt, U. and Perner, D.: Measurements of Atmospheric Trace Gases by Long Path Differential
UV/visible Absorption Spectroscopy, in: *Optical and Laser Remote Sensing*, edited by:
Killinger, D. K. and Mooradian, A., 95–105, Springer Verlag, New York, USA, 1983. 21374
- Platt, U. and Stutz, J.: *Differential Optical Absorption Spectroscopy, Physics of Earth and
30 Space Environments*. ISBN: 978-3-540-21193-8. Springer-Verlag Berlin Heidelberg, Ger-
many, 2008. 21374
- Rothman, L. S., Jacquemart, D., Barbe, A., Benner, D., Birk, M., Brown, L. R., Carleer, M. R.
C. C. J., Chance, K., Coudert, L. H., Dana, V., Devi, V. M., Flaud, J.-M., Gamache, R. R.,

The spatial distribution of the reactive iodine species IO

K. Seitz et al.

Title Page

Abstract

Introduction

Conclusions

References

Tables

Figures

⏪

⏩

◀

▶

Back

Close

Full Screen / Esc

Printer-friendly Version

Interactive Discussion



**The spatial
distribution of the
reactive iodine
species IO**K. Seitz et al.

[Title Page](#)[Abstract](#)[Introduction](#)[Conclusions](#)[References](#)[Tables](#)[Figures](#)[⏪](#)[⏩](#)[◀](#)[▶](#)[Back](#)[Close](#)[Full Screen / Esc](#)[Printer-friendly Version](#)[Interactive Discussion](#)

- Goldman, R., A., Hartmann, J.-M., Jucks, K. W., Maki, A. G., Mandin, J.-Y., Massie, S. T., Orphal, J., Perrin, A., Rinsland, C. P., Smith, M. A. H., Tennyson, J., Tolchenov, R. N., Toth, R., Auwera, J. V., Varanasi, P., and Wagner, G.: The HITRAN 2004 Molecular Spectroscopic Database, *J. Quant. Spectrosc. Rad. T.*, 96, 139–204, 2005. 21388
- 5 Saiz-Lopez, A. and Plane, J. M. C.: Novel iodine chemistry in the marine boundary layer, *Geophys. Res. Lett.*, 31, L04112, doi:10.1029/2003GL019215, 2004. 21373
- Saiz-Lopez, A., Plane, J. M. C., and Shillito, J. A.: Bromine oxide in the mid-latitude marine boundary layer, *Geophys. Res. Lett.*, 31, L03111, doi:10.1029/2003GL018956, 2004a. 21373
- 10 Saiz-Lopez, A., Saunders, R. W., Joseph, D. M., Ashworth, S. H., and Plane, J. M. C.: Absolute absorption cross-section and photolysis rate of I₂, *Atmos. Chem. Phys.*, 4, 1443–1450, 2004b. 21388
- Saiz-Lopez, A., Plane, J. M. C., McFiggans, G., Williams, P. I., Ball, S. M., Bitter, M., Jones, R. L., Hongwei, C., and Hoffmann, T.: Modelling molecular iodine emissions in a coastal marine environment: the link to new particle formation, *Atmos. Chem. Phys.*, 6, 883–895, 15 2006a. 21373
- Saiz-Lopez, A., Shillito, J. A., Coe, H., and Plane, J. M. C.: Measurements and modelling of I₂, IO, OIO, BrO and NO₃ in the mid-latitude marine boundary layer, *Atmos. Chem. Phys.*, 6, 1513–1528, 2006b. 21373, 21380
- 20 Saiz-Lopez, A., Plane, J. M. C., Mahajan, A. S., Anderson, P. S., Bauguitte, S. J.-B., Jones, A. E., Roscoe, H. K., Salmon, R. A., Bloss, W. J., Lee, J. D., and Heard, D. E.: On the vertical distribution of boundary layer halogens over coastal Antarctica: implications for O₃, HO_x, NO_x and the Hg lifetime, *Atmos. Chem. Phys.*, 8, 887–900, 2008, <http://www.atmos-chem-phys.net/8/887/2008/>. 21373
- 25 Sellegri, K., Yoon, Y. J., Jennings, S. G., O'Dowd, C. D., Pirjola, L., Cautenet, S., Chen, H., and Hoffmann, T.: Quantification of Coastal New Ultra-Fine Particles Formation from In situ and Chamber Measurements during the BIOFLUX Campaign, *Environ. Chem.*, 2, 260–270, 2005. 21376
- Simpson, W. R., von Glasow, R., Riedel, K., Anderson, P., Ariya, P., Bottenheim, J., Burrows, J., Carpenter, L. J., Frieß, U., Goodsite, M. E., Heard, D., Hutterli, M., Jacobi, H.-W., Kaleschke, L., Neff, B., Plane, J., Platt, U., Richter, A., Roscoe, H., Sander, R., Shepson, P., Sodeau, J., Steffen, A., Wagner, T., and Wolff, E.: Halogens and their role in polar boundary-layer ozone depletion, *Atmos. Chem. Phys.*, 7, 4375–4418, 2007,

<http://www.atmos-chem-phys.net/7/4375/2007/>. 21372

Spietz, P., Martin, J., and Burrows, J. P.: Spectroscopic studies of the I₂/O₃ photochemistry. Part 2. Improved spectra of iodine oxides and analysis of the IO absorption spectrum, *J. Photochem. Photobiol. A: Chem.*, 176, 50–67, 2005. 21388

5 Stein, T.: Application For Multi Axis Differential Optical Absorption Spectroscopy: From AMMAX To Halogene Measurements, Diploma thesis, Institut für Umweltphysik, Universität Heidelberg, Germany, 2006. 21378

Stutz, J. and Platt, U.: Numerical Analysis and Estimation of the Statistical Error of Differential Optical Absorption Spectroscopy Measurements with Least-Squares methods, *Appl. Opt.*, 35, 6041–6053, 1996. 21377

10 Stutz, J., Pikelnaya, O., Hurlock, S. C., Trick, S., Pechtl, S., and von Glasow, R.: Daytime OIO in the Gulf of Maine, *Geophys. Res. Lett.*, 34, L22816, doi:10.1029/2007GL031332, 2007. 21379, 21380

15 Vandaele, A. C., Hermans, C., Simon, P. C., Carleer, M., Colin, R., Fally, S., Merienne, M. F., Jenouvrier, A., and Coquart, B.: Measurements of the NO₂ absorption cross-section from 42000 cm⁻¹ to 10000 cm⁻¹ (238–1000 nm) at 220 K and 294 K, *J. Quant. Spectrosc. Rad. T.*, 59, 171–184, 1998. 21388

Voigt, S., Orphal, J., Bogumil, K., and Burrows, J. P.: The temperature dependence (203-293 K) of the absorption cross sections of O₃ in the 230-850 nm region measured by Fourier-transform spectroscopy, *J. Photochem. Photobiol.*, 143, 1–9, 2001. 21388

20 Voigt, S., Orphal, J., and Burrows, J. P.: The temperature and pressure dependence of the absorption cross-sections of NO₂ in the 250-800 nm region measured by Fourier-transform spectroscopy, *J. Photochem. Photobiol.*, 149, 1–7, 2002. 21388

von Glasow, R. and P. J. Crutzen, *Tropospheric Halogen Chemistry*, edited by: Holland, H. D. and Turekian, K. K., *Treatise on Geochemistry Update 1*, vol. 4.02, 1–67, 2007. 21372

25 Vuollekoski, H., Kerminen, V.-M., Anttila, T., Sihto, S.-L., Vana, M., Ehn, M., Korhonen, H., McFiggans, G., O'Dowd, C., and Kulmala, M.: Iodine dioxide nucleation simulations in coastal and remote marine environments, *J. Geophys. Res.*, 114, D02206, doi:10.1029/2008JD010713, 2009. 21373

**The spatial
distribution of the
reactive iodine
species IO**

K. Seitz et al.

Title Page

Abstract

Introduction

Conclusions

References

Tables

Figures

⏪

⏩

◀

▶

Back

Close

Full Screen / Esc

Printer-friendly Version

Interactive Discussion

**The spatial
distribution of the
reactive iodine
species IO**

K. Seitz et al.

Table 1. Differential absorption cross sections used for the analysis of the spectra.

Species	Reference
O ₄	Greenblatt et al. (1990)
NO ₂	Voigt et al. (2002)
I ₂	Saiz-Lopez et al. (2004b)
OIO	Bloss et al. (2001)
IO	Spietz et al. (2005)
H ₂ O	Rothman et al. (2005)
NO ₂ (MAX-DOAS)	Vandaele et al. (1998)
O ₃ (243 K, MAX-DOAS)	Bogumil et al. (2003)
O ₃ (223 K, MAX-DOAS)	Voigt et al. (2001)

[Title Page](#)[Abstract](#)[Introduction](#)[Conclusions](#)[References](#)[Tables](#)[Figures](#)[⏪](#)[⏩](#)[◀](#)[▶](#)[Back](#)[Close](#)[Full Screen / Esc](#)[Printer-friendly Version](#)[Interactive Discussion](#)

**The spatial
distribution of the
reactive iodine
species IO**

K. Seitz et al.

Table 2. Overview of the analysis settings

Species	Wavelength range [nm]	Polynomial [order]	Trace gas references applied
IO	416–448.5	5th	NO ₂
I ₂ /OIO	530–567	4th	NO ₂ , H ₂ O, O ₄
IO (MAX-DOAS)	414–438	3rd	O ₄ , NO ₂
I ₂ /OIO (MAX-DOAS)	553–567	3rd	O ₃ , H ₂ O, O ₄ , NO ₂

Title Page

Abstract

Introduction

Conclusions

References

Tables

Figures

I◀

▶I

◀

▶

Back

Close

Full Screen / Esc

Printer-friendly Version

Interactive Discussion

The spatial distribution of the reactive iodine species IO

K. Seitz et al.

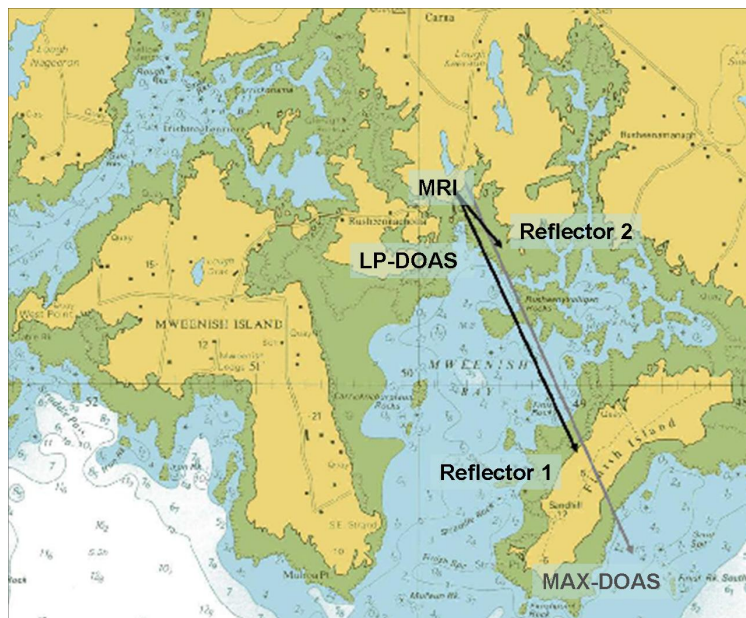


Fig. 1. Measurement site, the light paths of the active LP-DOAS are indicated in black arrows, the grey arrow indicates the viewing direction of the MAX-DOAS instruments.

© Crown Copyright and/or database rights. Reproduced by permission of the Controller of Her Majesty's Stationery Office and the UK Hydrographic Office (www.ukho.gov.uk).

[Title Page](#)

[Abstract](#)

[Introduction](#)

[Conclusions](#)

[References](#)

[Tables](#)

[Figures](#)

[⏪](#)

[⏩](#)

[◀](#)

[▶](#)

[Back](#)

[Close](#)

[Full Screen / Esc](#)

[Printer-friendly Version](#)

[Interactive Discussion](#)

The spatial distribution of the reactive iodine species IO

K. Seitz et al.

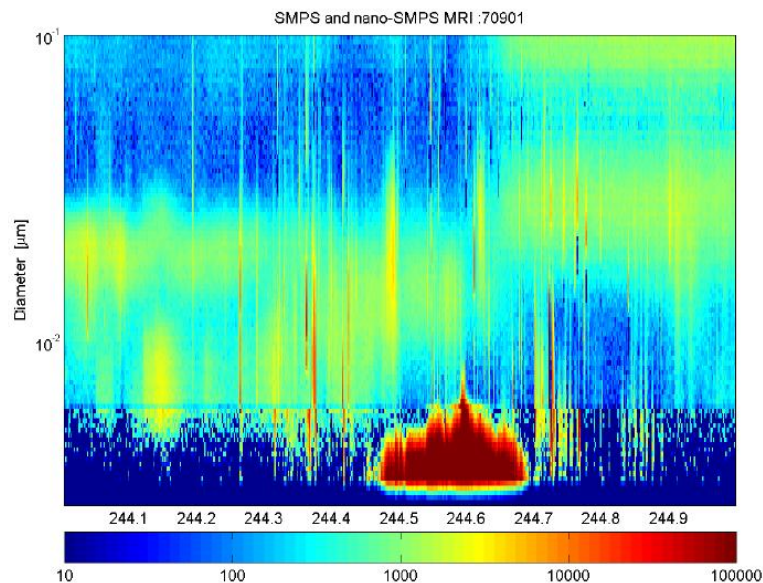


Fig. 2. Particle burst event measured 1 September (Julian date and time) with a nano-SMPS instrument. After noon particle concentrations up to 10^6 cm^{-3} particles were observed. The time of the event correlates well with low tide and high IO mixing ratios. (Particle data from T. Neary, University of Galway, personal communication, 2007)

Title Page

Abstract

Introduction

Conclusions

References

Tables

Figures

⏪

⏩

◀

▶

Back

Close

Full Screen / Esc

Printer-friendly Version

Interactive Discussion

The spatial distribution of the reactive iodine species IO

K. Seitz et al.

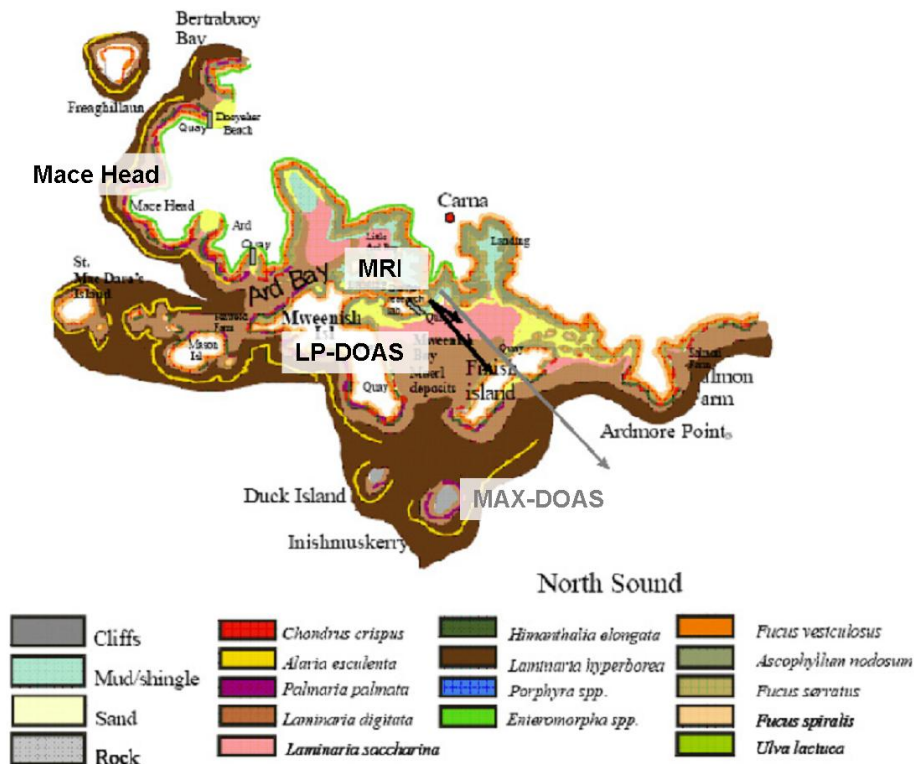


Fig. 3. Seaweed distribution in the vicinity of the MRI: Most of the seaweed is of the type *Laminaria*. The short light path crosses almost exclusively *Laminaria Saccharina*, whereas the long light path crosses first *Laminaria Saccharina* and then *Laminaria Digitata*. Adapted from [Connemara Seaweed Survey 2001. Irish Seaweed Centre, NUIG Internal report 72 pp.]

Title Page

Abstract

Introduction

Conclusions

References

Tables

Figures

◀

▶

◀

▶

Back

Close

Full Screen / Esc

Printer-friendly Version

Interactive Discussion

The spatial distribution of the reactive iodine species IO

K. Seitz et al.

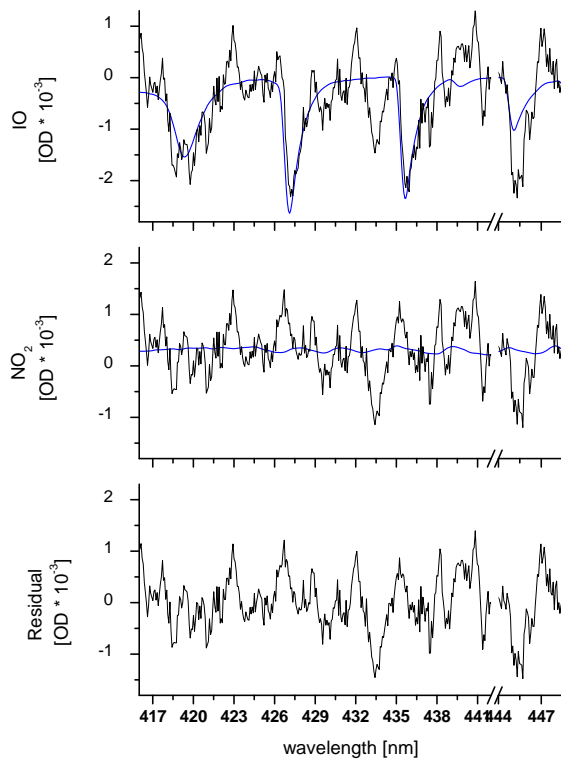


Fig. 4. Example for the spectral identification of IO on the long light path using the active LP-DOAS instrument. The spectrum was recorded 30 August 2007, 14:26 GMT. The corresponding mixing ratio of IO is 8.9 ± 0.86 ppt

Title Page

Abstract

Introduction

Conclusions

References

Tables

Figures

◀

▶

◀

▶

Back

Close

Full Screen / Esc

Printer-friendly Version

Interactive Discussion

The spatial distribution of the reactive iodine species IO

K. Seitz et al.

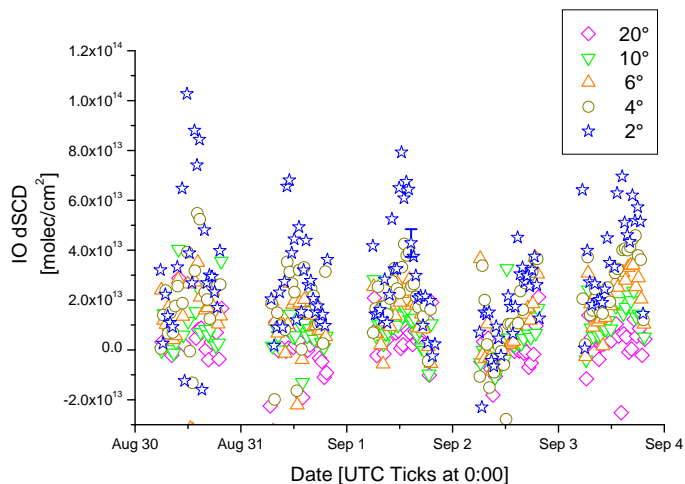


Fig. 5. IO dSCDs, different colors/symbols represent different elevation angles. A clear separation between different elevation angles can be seen with higher signals for lower angles, indicating a strong vertical gradient. For 1 September a typical error bar is given.

[Title Page](#)[Abstract](#)[Introduction](#)[Conclusions](#)[References](#)[Tables](#)[Figures](#)[◀](#)[▶](#)[◀](#)[▶](#)[Back](#)[Close](#)[Full Screen / Esc](#)[Printer-friendly Version](#)[Interactive Discussion](#)

The spatial distribution of the reactive iodine species IO

K. Seitz et al.

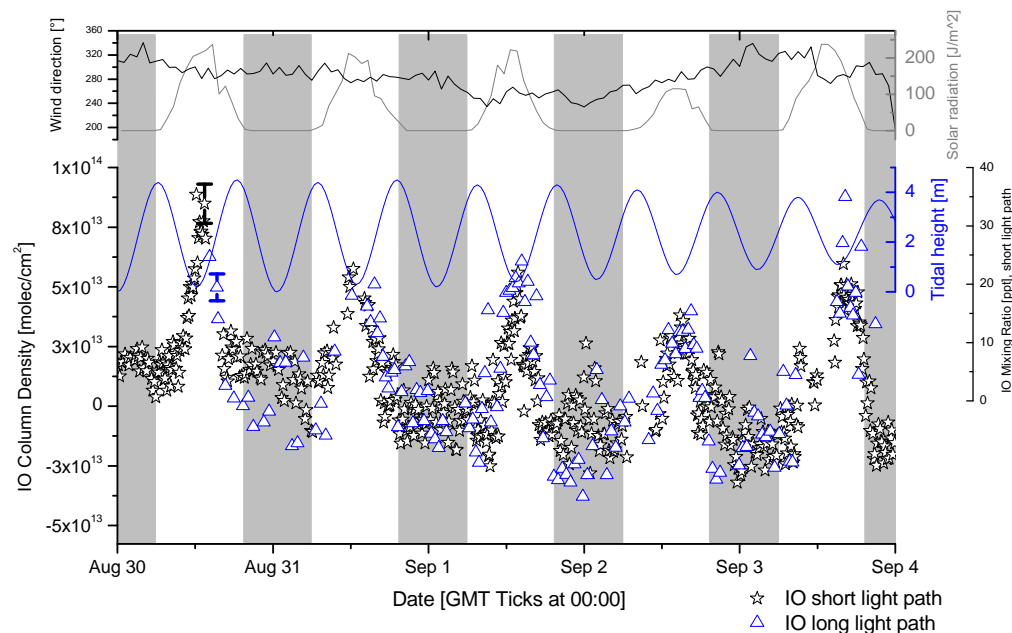


Fig. 6. Time series of IO on both active LP-DOAS light paths. The blue line indicates the tidal height and grey shaded areas mark periods of darkness. Blue triangles correspond to the IO column density seen over the short light path, black stars to the long light path. In the upper panels, solar radiation and wind direction are shown. The peaks in IO coincide with minima in tidal height and maxima in solar radiation. The column densities measured on both light paths are comparable indicating most of the IO signal originating in the intertidal area.

Title Page

Abstract

Introduction

Conclusions

References

Tables

Figures

◀

▶

◀

▶

Back

Close

Full Screen / Esc

Printer-friendly Version

Interactive Discussion

The spatial distribution of the reactive iodine species IO

K. Seitz et al.

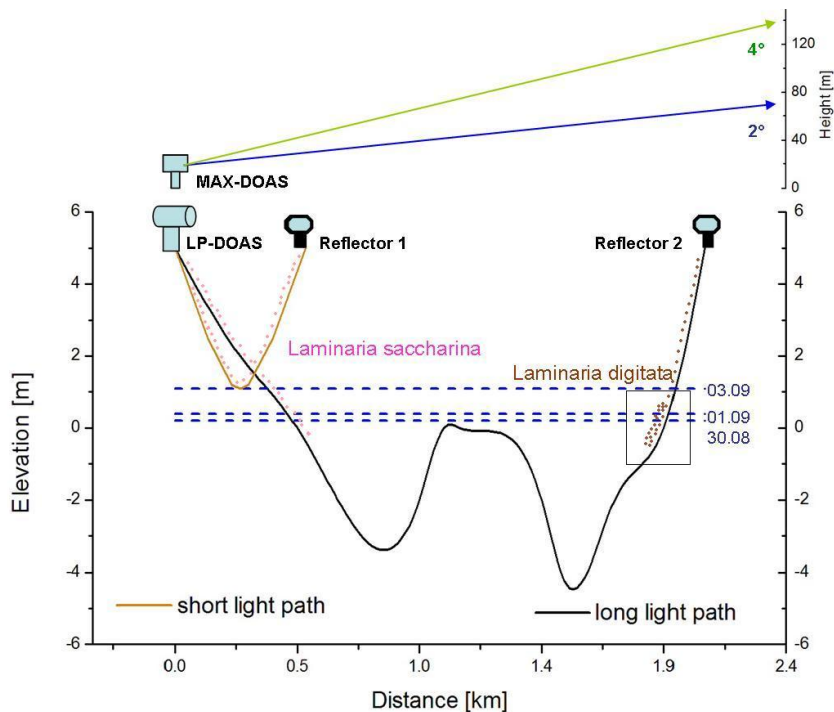


Fig. 7. Sketch of measurement set-up. Low tide water levels for 30 August, 1 and 3 September, 2007 are shown. The short light path crosses mainly *Laminaria Saccharina*, which are exposed during low tide for all days of measurement. The long light path crosses *Laminaria Saccharina* first and *Laminaria Digitata* on the other side of Mweenish Bay. Due to the steeper coast line on the other side of the bay, more seaweed is exposed along the long light path during periods of low spring tide (highlighted with box).

Title Page

Abstract

Introduction

Conclusions

References

Tables

Figures

◀

▶

◀

▶

Back

Close

Full Screen / Esc

Printer-friendly Version

Interactive Discussion

The spatial distribution of the reactive iodine species IO

K. Seitz et al.

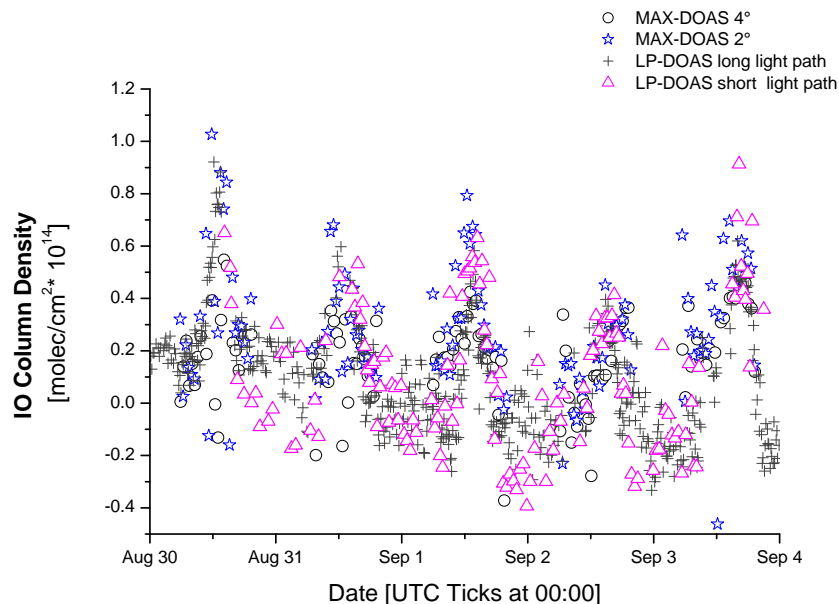


Fig. 8. Comparison of the column densities of the active LP-DOAS measurements with the differential slant column densities (dSCD) of the MAX-DOAS measurements at an elevation angle of 2° and 4°. (LP-DOAS column densities, short light path: pink triangles, long light path: black crosses; MAX-DOAS dSCDs, 2°: blue stars, 4°: black circles.)

[Title Page](#)[Abstract](#)[Introduction](#)[Conclusions](#)[References](#)[Tables](#)[Figures](#)[◀](#)[▶](#)[◀](#)[▶](#)[Back](#)[Close](#)[Full Screen / Esc](#)[Printer-friendly Version](#)[Interactive Discussion](#)

The spatial distribution of the reactive iodine species IO

K. Seitz et al.

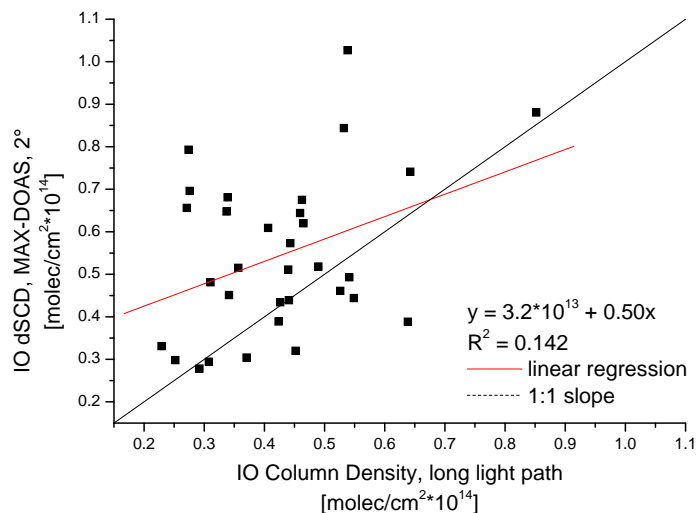


Fig. 9. Correlation between LP-DOAS (long light path) and 2° MAX-DOAS IO column densities. Column densities of the long light path were interpolated to the time grid of the MAX-DOAS measurements. Only data above the detection limit are shown.

Title Page

Abstract

Introduction

Conclusions

References

Tables

Figures

◀

▶

◀

▶

Back

Close

Full Screen / Esc

Printer-friendly Version

Interactive Discussion